# Solar wind-magnetosphere-ionosphere coupling: Neutral atmosphere effects on signal propagation

P. Song

Center for Atmospheric Research and Department of Environmental, Earth and Atmospheric Sciences, University of Massachusetts-Lowell, Lowell, Massachusetts, USA

V. M. Vasyliūnas

Max-Planck-Institut für Sonnensystemforschung, Katlenburg-Lindau, Germany

L. Ma

Center for Atmospheric Research and Department of Environmental, Earth and Atmospheric Sciences, University of Massachusetts-Lowell, Lowell, Massachusetts, USA

Received 15 March 2005; revised 27 May 2005; accepted 9 June 2005; published 23 September 2005.

[1] Waves that propagate between the outer magnetospheric regions (in particular the magnetopause or the magnetotail) and the ionosphere and thereby mediate the dynamic processes of the magnetosphere-ionosphere-thermosphere system are affected at the lower end of their paths by the interaction of the plasma with the neutral atmosphere. We use three-fluid equations (electrons, ions, and neutral particles) to study wave propagation and derive the general dispersion relation, under the simplifying assumptions of incompressible parallel propagation in a locally uniform system. Included are the effects of ion-neutral, electron-neutral, and ion-electron collisions on the electric current and on the plasma flow, as well as the effect of plasma-neutral collisions on the neutral atmospheric flow. At low frequencies, near and below the ion-neutral collision frequency, the properties of propagating perturbations are modified as a result of the interaction with the neutral atmosphere. Because the wavelengths may be too long for the local-uniformity assumption to apply, the quantitative statement of the modifications may not be reliable, but their qualitative properties are clear. Wave speed becomes substantially slower than the Alfvén speed because of inertia loading by neutrals. Waves are significantly damped because of plasma-neutral friction. Left-handed and right-handed waves have different dispersion properties because ion motion is inhibited much more than electron motion by collisions with neutrals. At still lower frequencies, below the neutral-ion collision frequency, plasma and neutrals move together, leading to wave speed equal to the Alfvén speed based on the total (plasma plus neutral) mass density and to disappearance of damping and of differences between left-handed and right-handed dispersions. These results indicate that the coupling of ionosphere and neutral atmosphere is better described as a (frictional) neutral-drag process rather than as Ohmic dissipation, in agreement with the conclusions of another direct study of energy equations in the ionosphere-atmosphere system.

**Citation:** Song, P., V. M. Vasyliūnas, and L. Ma (2005), Solar wind-magnetosphere-ionosphere coupling: Neutral atmosphere effects on signal propagation, *J. Geophys. Res.*, *110*, A09309, doi:10.1029/2005JA011139.

## 1. Introduction

[2] Much of magnetospheric dynamics is driven by inputs, both steady and variable, from the solar wind, and hence understanding the propagation of changes, on all spatial and temporal scales, from the magnetopause or from the magnetotail inward through the magnetosphere and down to the ionosphere is of central importance. As a first step in describing how an imposed change at the magnetopause or in the magnetotail (e.g., a sudden enhancement of reconnection) produces its signal at the ionosphere (via Fourier decomposition of the input, propagation of each frequency component at its own velocity, and Fourier reconstitution of the output), *Song and Vasyliūnas* [2002] developed a simple model of propagating imposed perturbations along magnetic field lines from the outer magnetosphere to the ionosphere. Although their model includes all frequency/time regimes, from near-speed-of-light propagation well above the plasma frequency to MHD waves well below the ion gyrofrequency, it assumes a collisionless plasma and hence is applicable in


0148-0227/05/2005JA011139

the spatial domain only to the magnetosphere, excluding the ionosphere.

[3] In this paper, we extend the physical model developed by *Song and Vasyliūnas* [2002] and add the effects of collisions between plasma and neutral particles, using collision rates appropriate to the ionosphere. The model is thus applicable continuously over the entire spatial range, from the magnetosphere down to and including all the layers of the ionosphere. The basis of the model is a three-fluid description, applicable to the partially ionized medium of the ionosphere-thermosphere system and including the collisionless magnetosphere as a limiting case: electrons, ions, and neutral particles, with interspecies collisions among all three included. Previously, *Song et al.* [2005] derived the three-fluid Ohm's law to describe the steady-state structure of the ionosphere coupled to the magnetosphere and the thermosphere, and with it they derived, for given magnetospheric boundary conditions, the continuous change of the plasma bulk velocity with height, from the magnetosphere to the lower ionosphere, as collisions become more and more important. Here we extend our previous work from steady state to wave propagation.

[4] Our analysis brings together several aspects which previously have been discussed mostly in isolation. A multifluid structured ionosphere has been treated in many ionospheric models [e.g., *Akasofu and DeWitt*, 1965; *Boström*, 1974; *Roble et al.*, 1998; *Kelley*, 1989; *Richmond et al.*, 1992], including attempts at describing time-dependent (but not wave) behavior for the closed field line regions of region 2 currents [e.g., *Peymirat et al.*, 1998]. Waves as an essential element in magnetosphere-ionosphere coupling have been treated by *Lysak* [1990, 1999], *Strangeway* [2002], and others, although the effects of the neutral motion on the wave propagations have not been included. Effects of neutral motion, on the other hand, on the high-frequency wave propagations have long been known in radio science [e.g., *Sen and Wyller*, 1960; *Booker*, 1984]. To the conventional magnetospheric description of magnetosphere-ionosphere coupling we add neutral atmosphere effects and a structured as well as dynamically responding ionosphere, to the (by now) conventional three-fluid treatment of the ionosphere we add time-dependent global propagation effects from the magnetopause, and to radio science we extend the neutral effects on wave propagation to lower frequencies. Although individual equations from the set we analyze have appeared in previous works, systematic application of the entire set over a broad frequency range appears to be novel. In particular, we are aware of no previous derivation of the complete dispersion relation for parallel propagation near and below the ion gyrofrequency.

[5] This is a very complicated physical/mathematical system, a realistic treatment of which remains a formidable task for the future. In this paper we obtain solutions for a highly idealized situation. We restrict ourselves to waves at a given frequency, leaving for future work the analysis of frequency and time integration. In section 2, we begin with the three-fluid treatment, three-fluid generalized Ohm's law, plasma momentum equation, and neutral momentum equation. We then apply these equations to the magnetosphere-ionosphere system, for now under the simplifying approximation of local uniformity. In section 3, we derive the (complex) dispersion relation for incompressible parallel propagation. The detailed derivation of the dispersion relation is given in Appendix A. In section 4, we focus on the low-frequency range and on parameters at some characteristic altitudes within the ionosphere, where most of the neutral-atmosphere effects on magnetosphere-ionosphere coupling occur, and calculate wave propagation and attenuation properties as functions of parameters at each height. In section 5, we give a simple physical interpretation of some remarkable wave properties described by the mathematical dispersion relation, discuss the relative roles of resistivity and neutral drag, and examine the applicability of the assumed locally uniform-medium approximation.

## 2. Three-Fluid Governing Equations

[6] A complete fluid treatment of three species, i.e., electrons, ions, and neutrals, can be obtained from the kinetic equations for each species by integrating these equations over the phase space, defining macroscopic quantities, and deriving the various moment equations for each species [e.g., *Sen and Wyller*, 1960; *Gombosi*, 1994; *Schunk and Nagy*, 2000]. These moment equations and macroscopic quantities describe each species as a fluid, without treating the motion of each individual particle. The momentum equations for the three species can be combined and rewritten as the generalized Ohm's law, the plasma momentum equation, and the neutral momentum equation [*Song et al.*, 2005]. They are

$$-\frac{m_e}{e}\frac{\partial \mathbf{j}}{\partial t} = -\nabla \bullet \mathbf{K}_e + \mathbf{j}\times\mathbf{B} - N_e e(\mathbf{E}+\mathbf{U}\times\mathbf{B}) + \mathbf{F}_e - N_e m_e(\nu_{en}-\nu_{in})(\mathbf{U}-\mathbf{u}_n) + \frac{m_e}{e}\left(\frac{m_e}{m_i}\nu_{in}+\nu_{en}+\nu_{ei}\right)\mathbf{j} + \frac{m_e}{m_i}\nabla\bullet\mathbf{K}_i - \frac{m_e}{m_i}\mathbf{F}_i, \quad (1)$$

$$m_i\frac{\partial N_e\mathbf{U}}{\partial t} = -\nabla\bullet\mathbf{K} + \mathbf{j}\times\mathbf{B} + \mathbf{F} - N_e(m_i\nu_{in}+m_e\nu_{en}) \cdot(\mathbf{U}-\mathbf{u}_n) + \frac{m_e}{e}(\nu_{en}-\nu_{in})\mathbf{j}, \quad (2)$$

$$m_n\frac{\partial N_n\mathbf{u}_n}{\partial t} = -\nabla\bullet\mathbf{K}_n + \mathbf{F}_n + \left(-\nabla\bullet\mathbf{K} + \mathbf{j}\times\mathbf{B} + \mathbf{F} - m_i\frac{\partial N_e\mathbf{U}}{\partial t}\right), \quad (3)$$

where $e$, $N_\eta$, $\mathbf{j}$, $\mathbf{U}$, $\mathbf{K}_\eta$, $\mathbf{E}$, $\mathbf{u}_n$, $\mathbf{B}$, $m_\eta$, and $\nu_{\eta\xi}$, are the elementary electric charge, the number density of species $\eta$, the electric current, the plasma bulk velocity, the kinetic tensor of particle species $\eta$, the electric field, the bulk velocity of neutrals, the magnetic field, the average mass of particles of species $\eta$, and the collision frequency between particles of species $\eta$ and $\xi$, respectively. The subscripts $i$, $e$, and $n$ denote ions, electrons, and neutrals, respectively. The vector $\mathbf{F}_\eta$ denotes all other forces exerted on species $\eta$, such as gravity, viscosity, and (if the equations are written in a rotating frame) centrifugal and Coriolis forces. $\mathbf{K} = \mathbf{K}_i + \mathbf{K}_e$ and $\mathbf{F} = \mathbf{F}_i + \mathbf{F}_e$. We assume, following the approximations discussed by *Song and Vasyliūnas* [2002], that the ions are

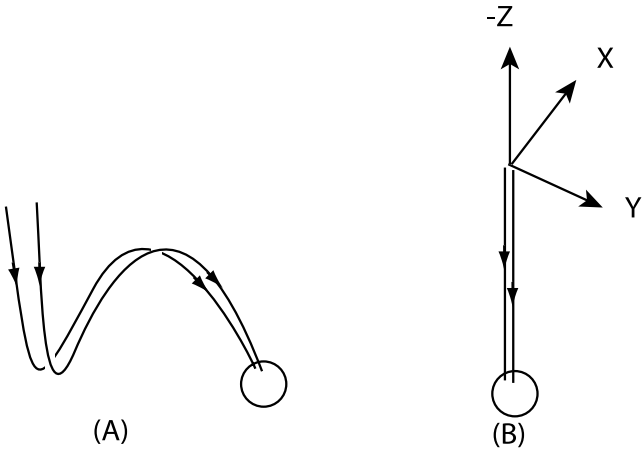


**Figure 1.** Reproduced from *Song and Vasyliūnas* [2002]. (a) Dayside open magnetic field lines viewed from afternoonside. (b) Simplified magnetic field lines.

singly charged, and that charge quasi-neutrality holds in the plasma, $N_e = N_i$. We have neglected possible wave-particle interactions, and we ignore photochemical processes (except, of course, insofar as they determine the height profile of the ionosphere).

[7] Equations (1), (2), and (3) describe the behavior of the current, plasma motion, and neutral wind, all important quantities in solar wind-magnetosphere-ionosphere coupling, and will be used as the basic equations in our work.

[8] We base our analysis on the physical model described by *Song and Vasyliūnas* [2002], as shown in Figure 1, in which perturbations propagate from the magnetopause to the ionosphere along the magnetic field, in regions without strong effects of Birkeland (field-aligned) currents and precipitating particles. As pointed out by Song and Vasyliūnas, the same model can also be used for perturbations on the nightside associated with magnetotail reconnection. Because we focus on electromagnetic coupling and collisions, we assume $\mathbf{F} = \mathbf{F}_n = 0$ and neglect compression. The incompressibility assumption combined with continuity and parallel propagation implies that the velocity perturbation is perpendicular to the propagation direction and that the gradient term $\nabla \cdot \mathbf{K}\eta$ vanishes. In this regard, we do not consider global scale ionospheric dynamo effects in our discussion.

[9] For simplicity, we treat the partially ionized gas system as locally uniform, i.e., we neglect the variation of plasma parameters with altitude and describe linear electromagnetic waves by a wave equation in which all the plasma parameters are treated as constants having their local values. Within each bounded domain of altitude, the dispersion relation (describing waves that can propagate up or down and can be reflected at boundaries) is thus approximated by that of a uniform medium with equivalent plasma parameters; the wave propagation properties change only implicitly with height, following the change of the parameters. (This approximation of a locally uniform medium is not to be confused with the assumption of an unbounded domain.)

[10] The local uniformity approximation is valid, in general, if the wavelength is much smaller than the spatial scale of the gradients of the plasma parameters. Since we are treating waves spanning a few orders of magnitude in frequency in a system of very large spatial scale, the approximation may not be valid everywhere and for all frequencies; in fact, it turns out to be rather poor for low-frequency waves in the ionosphere. In section 5.3, we discuss limits and corrections to the local uniformity approximation. Nevertheless, we will show that as a first step, many physical insights can be obtained from this physically simplest but mathematically still ponderous analysis.

[11] Even for a uniform system, the tightly coupled three-fluid equations are tedious to solve. Taking the parameters from Figure 1 of *Song et al.* [2001] and further assuming $\nu_e/\Omega_e \ll \nu_{in}/\Omega_i$ and $\nu_{in} \ll \nu_e$, where $\nu_e = \nu_{en} + \nu_{ei}$, we can simplify equations (1), (2), and (3) to

$$-\frac{m_e}{e}\frac{\partial \mathbf{j}}{\partial t} = \mathbf{j}\times\mathbf{B} - N_e e(\mathbf{E}+\mathbf{U}\times\mathbf{B}) - N_e m_e(\nu_{en}-\nu_{in})(\mathbf{U}-\mathbf{u}_n) + \frac{m_e}{e}\nu_e\mathbf{j}, \tag{4}$$

$$m_i\frac{\partial N_e\mathbf{U}}{\partial t} = \mathbf{j}\times\mathbf{B} - N_e m_i\nu_{in}(\mathbf{U}-\mathbf{u}_n) + \frac{m_e}{e}(\nu_{en}-\nu_{in})\mathbf{j}, \tag{5}$$

$$m_n\frac{\partial N_n\mathbf{u}_n}{\partial t} = \mathbf{j}\times\mathbf{B} - m_i\frac{\partial N_e\mathbf{U}}{\partial t}. \tag{6}$$

To complete the equation set, Maxwell equations are required: Faraday's law

$$\nabla\times\mathbf{E} = -\frac{\partial\mathbf{B}}{\partial t}, \tag{7}$$

and Ampère's law

$$\nabla\times\mathbf{B} = \mu_0\mathbf{j} + \frac{1}{c^2}\frac{\partial\mathbf{E}}{\partial t}. \tag{8}$$

The magnetic field is also divergence-free, from Maxwell equations. All quantities are to be evaluated using the local parameters.

## 3. Dispersion Relation and Propagation Velocities for Parallel Propagation

[12] We further follow the magnetosphere-ionosphere coupling model used by *Song and Vasyliūnas* [2002] to analyze the dispersion relations of different modes. What have been added to the model in this work are the neutral momentum equation and the collisions among the three species. Again, only incompressible parallel propagation modes are considered.

[13] Fourier-decomposing equations (4)–(8), under the assumption that the change in the magnetic field is much smaller than the background field, yields the dispersion relation for the system (detailed derivation in Appendix A),

$$\left[-\frac{\omega^2}{\Omega_e\Omega_i} \mp \frac{\omega}{\Omega_i} + 1 - (1+\alpha)\frac{(\nu_{en}-\nu_{in})^2}{\Omega_e^2} + (1+\alpha)\frac{\nu_{in}\nu_e}{\Omega_e\Omega_i}\right] + i\left[\frac{\omega\nu_e}{\Omega_e\Omega_i} + (1+\alpha)\frac{\omega\nu_{in}}{\Omega_i\Omega_e} \pm (1+\alpha)\frac{\nu_{in}}{\Omega_i} \mp 2\frac{(\nu_{en}-\nu_{in})}{\Omega_e} - \frac{\nu_{in}}{\omega}\alpha\right] = \left(\frac{\omega_{pe}^2}{\Omega_i\Omega_e}\right)\frac{1}{(n^2-1)}\left[1 - i(1+\alpha)\frac{\nu_{in}}{\omega}\right] \tag{9}$$

**Table 1.** Three Cases With Different Collision Frequencies

| | A | B | C |
|---|---|---|---|
| $\nu_{ei}/\Omega_i$ | 0.01 | 1 | 100 |
| $\nu_{en}/\Omega_i$ | 0.01 | 1 | 100 |
| $\nu_{in}/\Omega_i$ | 0.01 | 1 | 100 |
| $\alpha$ | $1 \times 10^{-4}$ | $1 \times 10^{-4}$ | $1 \times 10^{-4}$ |
| $V_A$, km/s | 1000 | 1000 | 1000 |
| $a_i$ | 16 | 16 | 16 |

where $n = kc/\omega$ is the index of refraction, $k$ and $\omega$ are the wave number and frequency, and $\alpha = m_i N_e / m_n N_n$ is the total mass density ratio of the plasma to neutrals. (No assumptions have been made about the order of magnitude of $\alpha$.) Because of collisions, the index of refraction and the wave number are now complex, $n = n_R + in_I$ and $k = k_R + ik_I$. The reciprocal of the imaginary part of the wave number, $1/k_I$, gives the attenuation depth of the wave: the distance over which the wave amplitude is reduced, when $k_I$ is negative, by a factor $1/e$. The phase velocity is defined as $V_{phase} = c/n_R = \omega/k_R$. The group velocity may be defined as $V_{group} = (dk_R/d\omega)^{-1}$. In the presence of attenuation (nonzero $k_I$), however, its physical significance is limited, and in particular it is not generally the same as the signal propagation velocity (cf. discussion by *Brillouin* [1960]).

[14] The dispersion relation depends strongly on the ratios of collision frequencies to gyrofrequencies and on the mass-density ratio of plasma to neutrals. Strictly speaking, these two quantities are not completely independent: for given ionospheric parameters (electron concentration, magnetic field) and atomic-physics quantities (particle charges and masses, collision cross sections), the collision frequency and $1/\alpha$ both vary in proportion to $n_n$. Nevertheless, they enter equation (9) for different physical reasons: the collision frequency terms come from the effect of collisions on charged particle motion, and the $\alpha$ terms come from the effect of the same collisions on neutral particle motion. It is instructive to separate the two effects, and for this purpose we first examine three cases (parameters given in Table 1) with the same density ratio but different collision frequencies. Figure 2 shows the dispersion relations, the frequency versus the real part of the wave number, for the three cases. The two panels from top are for the left-hand and right-hand modes, respectively. (Note: "left-hand" and "right-hand" are here defined by reference to the mean magnetic field direction, as customary in plasma physics, and not to the direction of propagation, as in optics and conventional electromagnetics. Left-hand or right-hand waves rotate in the direction of gyration of ions or electrons, respectively; their circular polarization, in the conventional sense, is that of their name if the propagation and the mean field directions are parallel but is reversed if antiparallel.) Changes at characteristic frequencies $\omega_{pe}$, $\Omega_e$, $\Omega_i$, $\nu_{in}$, $\alpha\Omega_i$, and $\alpha\nu_{in}$ are evident. Notice that the density ratio effects appear at $\alpha\Omega_i$ for the high-collision case and at $\alpha\nu_{in}$ for the low-collision case. Figure 3 shows the dispersion relations evaluated using the parameters of the ionosphere at 100 km,

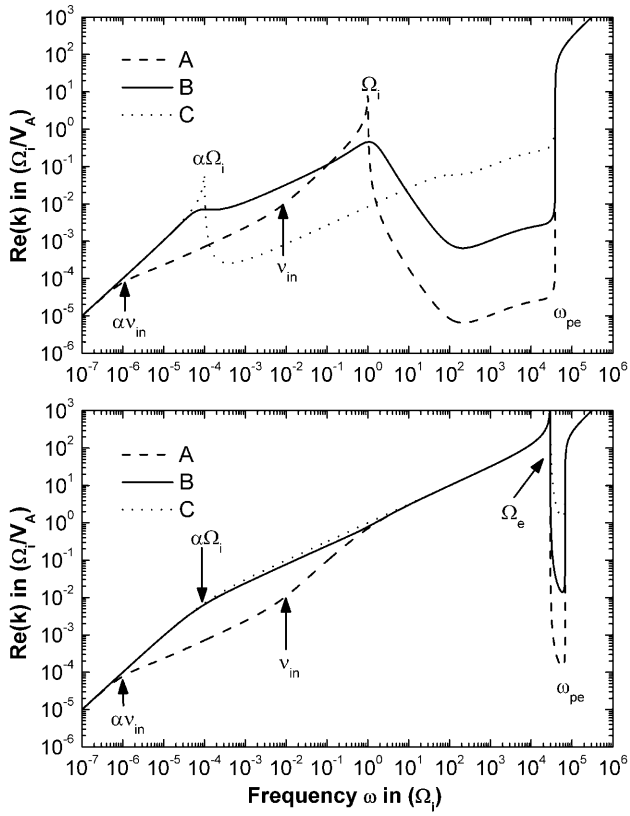


**Figure 2.** Dispersion relations for three-fluid collisional system for three sets of collision frequencies using parameters given in Table 1. The upper (lower) panel is for the left- (right-) hand modes.

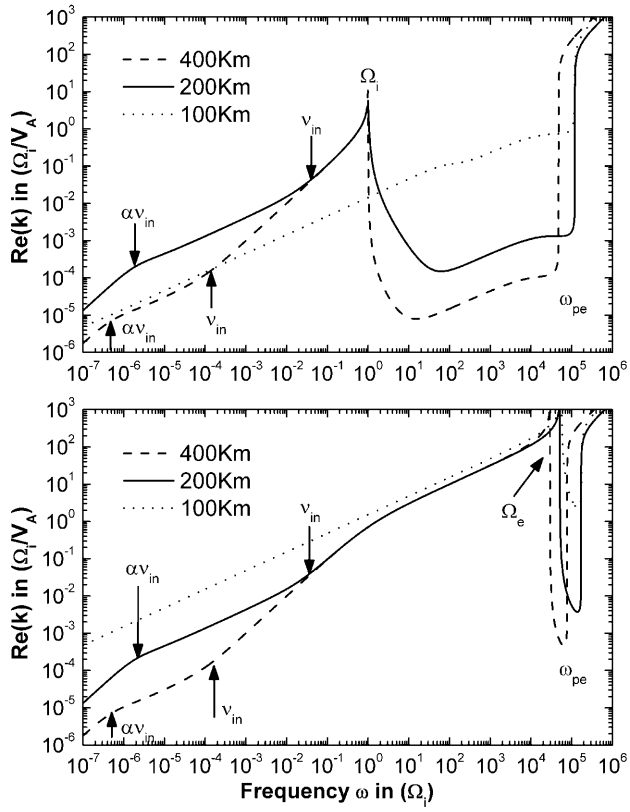


**Figure 3.** Dispersion relations using parameters given in Table 2, corresponding to those in the ionosphere at altitudes of 100 km, 200 km, and 400 km. The upper (low) panel shows the left- (right-) handed polarized modes.

**Table 2.** Ionospheric Parameters Near Dayside Cusp

| | Height, km | | |
|---|---|---|---|
| | 100 | 200 | 400 |
| $\Omega_i$, $s^{-1}$ | 178 | 187 | 297 |
| $\nu_{ei}/\Omega_i$ | 5.05 | 0.656 | 0.084 |
| $\nu_{en}/\Omega_i$ | 542 | 0.806 | 0.0023 |
| $\nu_{in}/\Omega_i$ | 108 | 0.035 | 0.00017 |
| $\alpha$ | $7.0 \times 10^{-9}$ | $5.7 \times 10^{-5}$ | $3.1 \times 10^{-3}$ |
| $V_A$, km/s | 758 | 474 | 849 |
| $a_i$ | 31 | 28 | 16 |

200 km, and 400 km, as given in Table 2, which is derived from Figure 1 of *Song et al.* [2001]. Note that the height given for each line is the height at which the densities and frequencies have been evaluated, and hence the lines cannot be interpreted as the time sequence of a wave. We have omitted the frequency range much higher than the plasma frequency; waves in this range have been studied extensively by the radio wave propagation community [e.g., *Sen and Wyller*, 1960].

[15] In the near-Earth environment, the gyrofrequency and collision frequency vary over a large range of values: the difference between the two gyrofrequencies is between 3 and 4 orders of magnitude (taking into account the change of the average ion atomic weight from 1 at high altitudes to about 16 in the ionosphere), $\nu_{en} \ll \Omega_e$ above 80 km, the difference between the ion-neutral and electron-neutral collision frequencies is about 1 to 3 orders of magnitude, and $\alpha$ is about $10^{-2\sim-10}$. Under these conditions, equation (9) can be simplified to

$$\left[-\frac{\omega^2}{\Omega_e\Omega_i} \mp \frac{\omega}{\Omega_i} + 1 + \frac{\nu_{in}\nu_e}{\Omega_e\Omega_i}\right] + i\left[\frac{\omega\nu_e}{\Omega_e\Omega_i} \pm \frac{\nu_{in}}{\Omega_i} - \frac{\nu_{in}}{\omega}\alpha\right] = \left(\frac{\omega_{pe}^2}{\Omega_i\Omega_e}\right)\frac{1}{(n^2-1)}\left(1 - i\frac{\nu_{in}}{\omega}\right) \quad (10)$$

There are two limiting situations: weak collision when $\nu_{in} \ll \nu_e \ll \Omega_i \ll \Omega_e$ and strong collision when $\Omega_i \ll \nu_{in} \ll \nu_e \ll \Omega_e$. These correspond roughly to regions above 250 km and between 90 km and 250 km, respectively, as shown in Figure 1 of *Song et al.* [2001]. In the weak-collision regions where the collision frequencies are much smaller than the ion gyrofrequency, the dispersion is, except at frequencies below $\alpha\nu_{in}$, similar to that in a collisionless plasma which has been discussed in detail by *Song and Vasyliūnas* [2002]. In the frequency band between the ion and the electron gyrofrequencies, the left-hand mode does not propagate in a collisionless plasma but does propagate when collisions are included (see upper panel of Figures 2 and 3), albeit with strong attenuation (see section 4.3).

## 4. Low-Frequency Propagation Near and in the Ionosphere

### 4.1. Low-Frequency Limit

[16] When a wave propagates from the magnetopause or magnetosphere to the ionosphere, its frequency in absolute units remains the same but the ratio of wave frequency to gyrofrequency decreases because of the increase in the ambient field strength; hence the wave in effect shifts to a lower-frequency range in the dispersion relation. A whistler mode wave at the magnetopause may thus become an MHD wave when it has propagated down to the ionosphere. It is safe to assume that all waves generated at the magnetopause with significant power become whistler and MHD modes in the ionosphere because of a two-order increase in the ion gyrofrequency and a less than two-order increase in the plasma frequency. Depending on how sharp the onset of reconnection is, the power may be distributed over a large range of frequencies. Although high-frequency waves may carry a significant portion of the power, they carry less (time-integrated) energy and their dynamic effects are less important. Here we note that in the problem we are treating, the source of the perturbations diminishes after the reconnection onset and we study only the transient dynamic processes. Lower frequencies carry more total energy and produce long-lasting effects. Although we discuss simplified forms of different quantities in this section, the numerical results shown are based on the complete forms.

[17] We focus on the lower-frequency range, corresponding to periods from a few seconds to less than 2 hours, or $10^1 \sim 10^{-3}$ $s^{-1}$ in angular frequency. Close to the Earth, in this frequency range, we have $\omega \ll \Omega_i \sim 10^{2}$ $s^{-1} \ll \Omega_e$, but the collision frequencies may be either greater or smaller than the wave frequency. For these low-frequency waves, equation (10) becomes

$$(1+\kappa) + i\left(\frac{\omega}{\nu_{in}}\kappa \pm \frac{\nu_{in}}{\Omega_i} - \frac{\nu_{in}}{\omega}\alpha\right) = \left(\frac{\omega_{pe}^2}{\Omega_i\Omega_e}\right)\frac{1}{(n^2-1)}\left(1 - i\frac{\nu_{in}}{\omega}\right), \quad (11)$$

where $\kappa = \nu_{in}\nu_e/\Omega_i\Omega_e$.

### 4.2. Propagation Speed

[18] Solving for the real part of the index of refraction in equation (11) gives the phase velocity

$$V_{ph}^2 = 2V_A^2\frac{P}{Q}\left[1 + \left(1 + \frac{T^2}{Q^2}\right)^{1/2}\right], \quad (12)$$

where

$$P = (1+\kappa)^2 + \left(\frac{\omega}{\nu_{in}} \pm \frac{\nu_{in}}{\Omega_i} - \frac{\nu_{in}}{\omega}\right)^2, \quad (13)$$

$$Q = 1 \mp \frac{\nu_{in}^2}{\omega\Omega_i} + \frac{\nu_{in}^2}{\omega^2}\alpha, \quad (14)$$

$$T = -\frac{\nu_{in}}{\omega}(1+\kappa) - \frac{\omega}{\nu_{in}}\kappa. \quad (15)$$

Figures 4 and 5 show the phase velocities in the frequency range of interest based on the parameters given in Tables 1 and 2, respectively. They are derived from the complete dispersion relation (9) but shown for a smaller frequency range. In the weak-collision cases, at frequencies much below the ion gyrofrequency, the phase velocity remains nearly constant at the Alfvén speed until the frequency decreases to the ion-neutral collision frequency. The phase velocity then decreases with decreasing frequency $\omega$ and

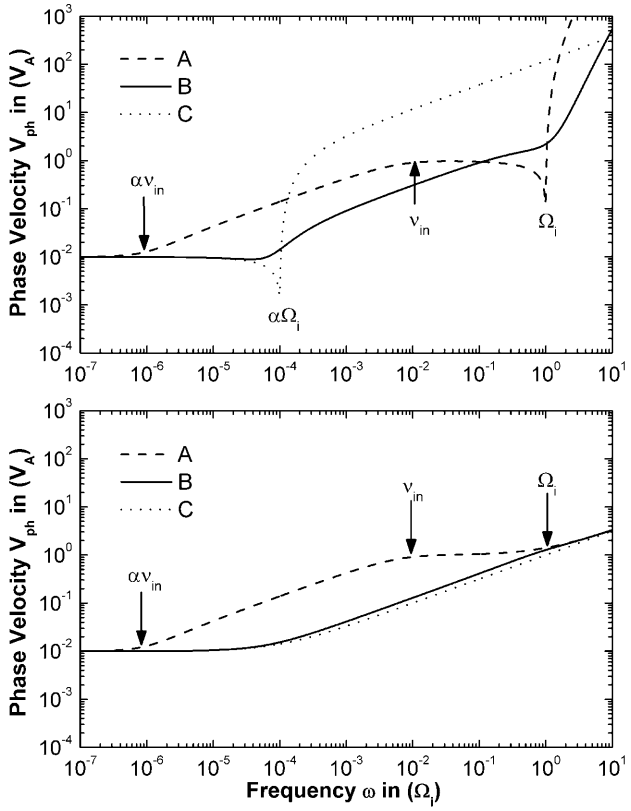


**Figure 4.** Phase velocities for the two modes using the same sets of the parameters as Figure 2 and Table 1.

reaches a constant speed of $\alpha^{1/2}V_A$ for $\omega \ll \alpha\nu_{in}$. For high-collision cases, the phase velocity decrease begins at the (higher) electron collision frequency and reaches its asymptotic value of $\alpha^{1/2}V_A$ for $\omega$ below $\alpha\Omega_i$.

[19] Figure 6 compares the effects of collision and neutral drag. Without neutral collisions ($\nu_{in} = \nu_{en} = 0$, dashed lines), the lower-frequency waves of the left-hand mode propagate at the Alfvén speed with an upper cutoff at the ion gyrofrequency, as in conventional plasma theory. The right-hand mode propagates at the whistler speed (Alfvén speed) in frequencies above (below) the ion gyrofrequency. With collisions but with an unmoving thermosphere ($\alpha = 0$, dotted lines), the right-hand mode extends the whistler mode dispersion to lower frequencies. The left-hand mode can propagate at frequencies above the ion gyrofrequency, and at lower frequencies the wave speed continuously decreases with decreasing frequency in a similar manner as the whistler mode. With collisions as well as with a self-consistently coupled motion of the thermosphere (solid lines), the wave speed for both modes at the lowest frequencies reaches a constant value of $\alpha^{1/2}V_A$, as discussed above.

[20] The decrease of the phase velocity with decreasing frequency can be understood as the result of the following neutral-inertia-loading process. For the low-collision case, when $\omega$ is much higher than $\nu_{in}$, no collisions occur during a wave cycle and the wave propagates in essentially the same way as in a collisionless plasma. When the frequency is less than the ion-neutral collision frequency $\nu_{in}$, ions collide with neutrals during a wave cycle, tending to make the neutrals move with the bulk of ions for $\omega \ll \Omega_i$. This is equivalent to adding some neutral inertia to the motion of the field line. The fraction of the neutrals that oscillate with the ions and hence move with the field line increases as the frequency decreases further, and when $\omega \ll \alpha\nu_{in}$ every neutral in effect oscillates with the wave. The mass density on the field line then becomes $m_nN_n + m_iN_i \sim m_nN_n = m_iN_i/\alpha$, and the phase velocity is the equivalent Alfvén speed based on the neutral mass density, giving the factor $\alpha^{1/2}$. Since $\alpha \sim 10^{-3\sim-8}$, the phase velocity can be $10^{-1.5\sim-4}$ times smaller than the $V_A \sim$700 km/s, i.e., $v_{ph}$ can be of the order of $10^{-1\sim1.5}$ km/s. As $\alpha$ decreases rapidly at lower altitudes, the waves propagate more slowly into the ionosphere.

### 4.3. Wave Attenuation

[21] In addition to slowing down the propagation, another, more widely known, major effect of the neutrals is to attenuate the perturbations. The attenuation rate is conventionally defined as the ratio of the imaginary part to the real part of the wave number and is thus proportional to the logarithmic decrease of amplitude over one wavelength.

[22] Figure 7 shows the attenuation rate as a function of frequency, for the two modes and at three heights. Significant attenuation (rate $\sim$1) occurs at frequencies from $\omega \sim \nu_{in}$ down to about $\alpha\Omega_i$ or $\alpha\nu_{in}$, whichever is smaller. The left-hand mode is in addition very heavily attenuated at frequencies above $\Omega_i$ (where it does not propagate at all in the absence of collisions). Except at $\omega$ near and above $\Omega_i$,

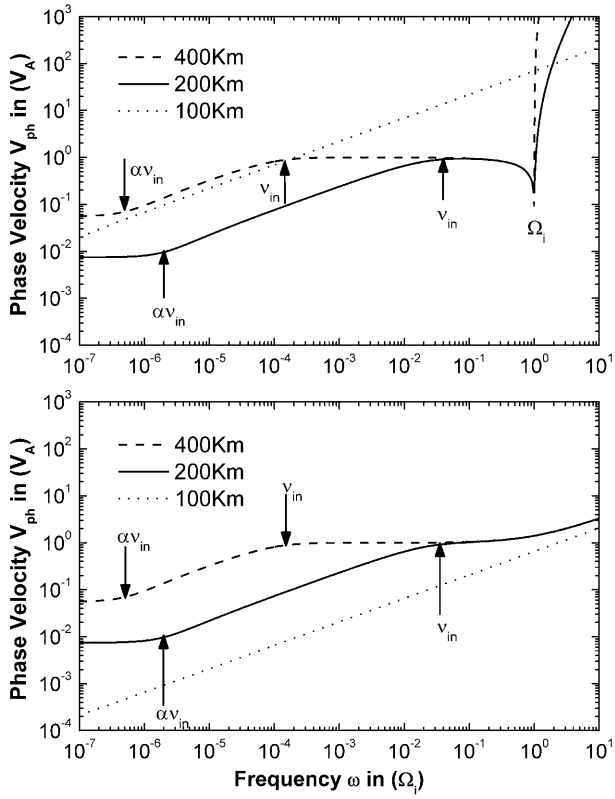


**Figure 5.** Phase velocities for the two modes at three heights using the same set of the parameters as Figure 3 and Table 2.

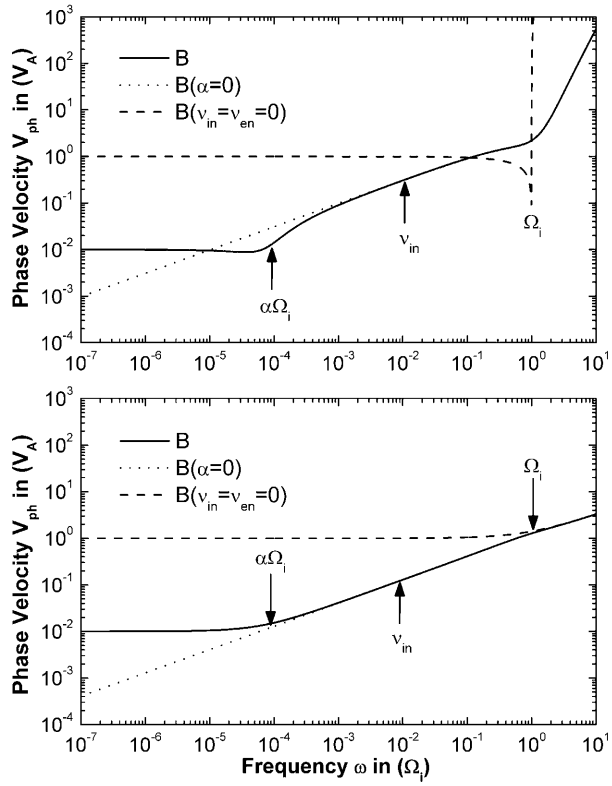


**Figure 6.** Comparison of the effects of collisions and neutral drag. The solid lines show the results using the parameters for case B given in Table 1. The dashed (dotted) lines show the results for the same case but let collision frequencies ($\alpha$) be zero.

there is little difference between the two modes at heights of 200 km and above. At 100 km, on the other hand, the attenuation is very heavy (rate ~100) for the left-hand mode and very slight (rate ~0.01) for the right-hand mode.

[23] The attenuation rate, although widely used in plasma physics, does not tell the complete story for our purpose because the attenuation occurs only over a finite height range in the ionosphere. Even when the attenuation rate per wavelength is large, the wave may cross the ionosphere with small total attenuation, provided the wavelength is much longer than the thickness of the ionosphere. The more relevant physical quantity is thus the attenuation depth $D = 1/k_I$, the absolute distance (regardless of wavelength) over which the wave amplitude decreases by a factor $1/e$. When $D$ is smaller than the thickness of the ionosphere, the wave is effectively absorbed in the ionosphere, but if $D$ is much greater than the thickness of the ionosphere, the wave propagates across it with little change in amplitude.

[24] Figure 8 shows the attenuation depth as function of frequency for the two modes and three heights. In general, the attenuation lengths are about the same for both modes, with the exception of the lowest height (100 km) for all frequencies and of $\omega$ near and above $\Omega_i$ for all heights, where the attenuation length is shorter by two or more orders of magnitude for the left-hand mode. At 100 km, the scaled unit for the vertical axis corresponds to about 1 km. From Figure 8 it then follows that the right-hand mode can cross the ionosphere at nearly all frequencies with little or no attenuation, but the left-handed mode can do so only when its frequency is less than about 0.1 Hz, otherwise being heavily attenuated at the lowest heights.

### 4.4. Signal Arrival Time

[25] As discussed, e.g., by *Song and Vasyliūnas* [2002], when reconnection turns on for a limited time at the magnetopause or the magnetotail, perturbations at all frequencies propagate downward, arriving eventually at the ionosphere. The first major wave front, arriving in about 2 min if the field line is about 16 $R_E$ long, is the conventional MHD front which corresponds to the arrival of the plasma flow and magnetic field perturbations. Describing in detail the signal arrival time effects of and on the neutral atmosphere requires both generalizing the group velocity concept to allow for attenuation [*Brillouin*, 1960] and considering departures from local uniformity and thus lies beyond the scope of this paper. We note merely that neutral effects at low altitudes occur on longer timescales. In particular, the neutral wind begins to be affected by the magnetospheric driver on timescales of $1/\nu_{in}$ and can reach nearly full convection with the plasma on timescales of about $1/\alpha\nu_{in} \sim 2-3$ hours. If the reconnection process does not last that long, the neutral wind will not be driven or will be only partially driven. The neutral wind is thus substantially driven by the magnetosphere on timescales of a fraction of $1/\alpha\nu_{in}$. On longer timescales, other mechanisms that may limit the neutral wind speed and prevent it from

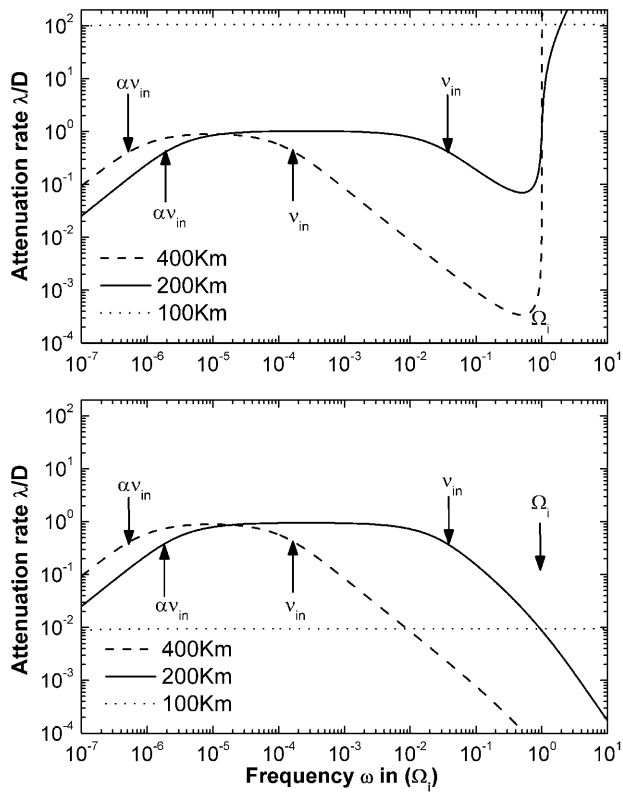


**Figure 7.** Attenuation rates, $k_I/k_R$, for the two modes at three heights using the same sets of the parameters as Figure 3 and Table 2.

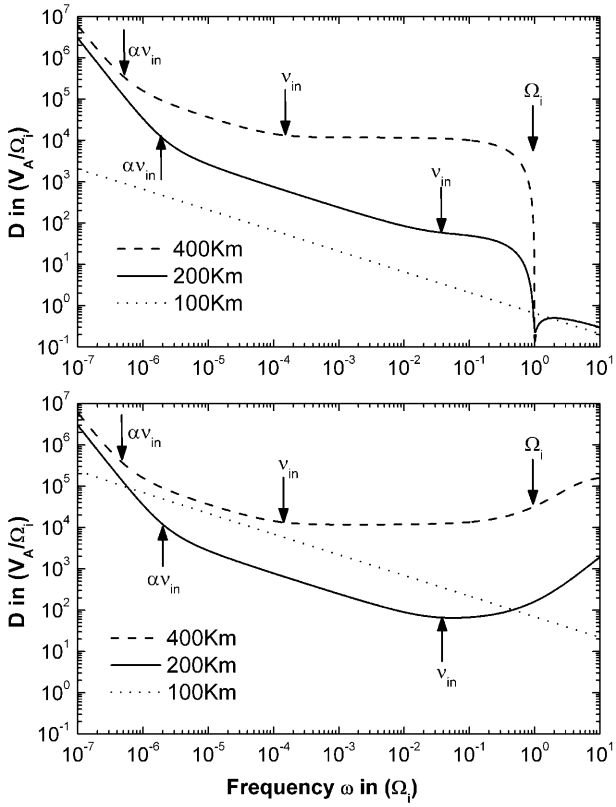


**Figure 8.** Attenuation depths, $D$, for the two modes at three heights using the same set of the parameters as Figure 3 and Table 2.

moving with the plasma (allowing for possibly supersonic relative motion of plasma and neutrals) need to be included.

## 5. Discussion

### 5.1. Physical Description of Wave Properties in the Highly Collisional Regime

[26] The properties of the waves derived in the preceding section, although straightforward consequences of the mathematical development, display some aspects in the highly collisional limit $\nu_{in} \gg \Omega_i$ ("C" and "100 km" curves in Figures 2–5) that perhaps are not intuitively obvious. One is the various characteristic frequencies, at or near which the dispersions curves change. The significance of $\Omega_i$, $\nu_{in}$, and $\alpha\nu_{in} = \nu_{ni}$ is clear, but what is special about $\omega = \alpha\Omega_i$, and only for the left-hand mode? To study this, we simplify the plasma and neutral momentum equations to

$$\frac{\partial \mathbf{U}}{\partial t} = \frac{1}{N_e m_i}\mathbf{j} \times \mathbf{B} - \nu_{in}(\mathbf{U} - \mathbf{u}_n), \tag{16}$$

and

$$\frac{\partial \mathbf{u}_n}{\partial t} = \alpha\nu_{in}(\mathbf{U} - \mathbf{u}_n). \tag{17}$$

and further rewrite equation (16) by replacing the $\mathbf{j} \times \mathbf{B}$ term from the generalized Ohm's law as

$$\frac{\partial \mathbf{U}}{\partial t} = \Omega_i \mathbf{b} \times (\mathbf{U}_B - \mathbf{U}) - \nu_{in}(\mathbf{U} - \mathbf{u}_n), \tag{18}$$

where $\mathbf{b}$ is the unit vector along $\mathbf{B}$ and $\mathbf{U}_B = \mathbf{E} \times \mathbf{B}/B^2$. For a wave of frequency $\omega$ in the left-hand or right-hand mode as defined in section 3, the time derivative of any transverse vector $\mathbf{V}$ is

$$\frac{\partial \mathbf{V}}{\partial t} = -\sigma\omega \mathbf{b} \times \mathbf{V}, \tag{19}$$

where $\sigma = +1$ $(-1)$ for the left-hand (right-hand) mode. (This is simply the statement that the vector rotates as described. Note that throughout this section we are using real quantities instead of complex Fourier amplitudes.) With the use of relation (19), the neutral momentum equation (17) becomes

$$-\sigma\omega \mathbf{b} \times \mathbf{u}_n = \nu_{ni}(\mathbf{U} - \mathbf{u}_n) \tag{20}$$

and the plasma equation (18) can be rewritten (with the further simplification of neglecting $\omega$ compared to $\Omega_i$)

$$\Omega_i \mathbf{b} \times \mathbf{U} = -\nu_{in}(\mathbf{U} - \mathbf{u}_n) + \Omega_i \mathbf{b} \times \mathbf{U}_B \tag{21}$$

Equations (20) and (21) can be solved for the difference $\mathbf{U} - \mathbf{u}_n$:

$$\mathbf{U} - \mathbf{u}_n = \frac{\mathbf{U}_B - \xi \mathbf{b} \times \mathbf{U}_B}{1 + \xi^2} \tag{22}$$

where

$$\xi = \frac{\nu_{ni}}{\sigma\omega} - \frac{\nu_{in}}{\Omega_i} = \frac{\nu_{in}}{\Omega_i}\left(\frac{\alpha\Omega_i}{\sigma\omega} - 1\right) \tag{23}$$

At the value $\xi = 0$, the velocity difference $\mathbf{U} - \mathbf{u}_n$ assumes its maximum value, and its component perpendicular to $\mathbf{U}_B$ (parallel to $\mathbf{E}$) reverses sign. $\xi = 0$, however, can occur only for $\sigma = +1$ (left-hand mode) and implies the condition $\omega = \alpha\Omega_i$. In essence this is a match between the ratio of collision to rotation terms: $\nu_{ni}/\omega$ for neutrals and $\nu_{in}/\Omega_i$ for ions.

[27] The other striking result in the highly collisional limit is the large difference, by one or two orders of magnitude, in the dispersion relations for the left-hand and the right-hand modes. Normally, the modes differ much only at frequencies between $\Omega_i$ and $\Omega_e$, where the different gyromotions of electrons and ions result in different responses to the wave fields. In the MHD regime, where the gyroperiod of either is very short compared to the wave period, both modes propagate at the same Alfvén speed in the collisionless limit. Collisions with neutrals change the two modes differently, not because of anything to do with gyromotion but because they affect ions much more than electrons. For disturbances propagating with wave vector $\mathbf{k}$ along the $\mathbf{b}$ direction and obeying the polarization condition (19), the spatial and temporal derivatives are related by

$$\frac{\partial}{\partial z} = -\frac{\mathbf{k} \bullet \mathbf{b}}{\omega}\frac{\partial}{\partial t}$$

(we ignore an additional term due to attenuation, which plays no role in our argument). For the assumed geometry,

Ampère's-law relation between the disturbance magnetic field $\delta\mathbf{B}$ and the current density $\mathbf{j}$ takes the form

$$-\sigma(\mathbf{k}\bullet\mathbf{b})\delta\mathbf{B}=\mu_0\mathbf{j}. \tag{24}$$

In the collisionless regime, $\mathbf{j}$ is related by the plasma momentum equation to the time derivative of $\mathbf{U}$, giving with the aid of equation (19)

$$\mathbf{j}=-\sigma\omega\frac{N_e m_i}{B}\mathbf{U} \tag{25}$$

In the collisional regime, on the other hand, the ion flow is greatly impeded by collisions with neutrals while the electrons remain (even in what for our purposes is a highly collisional parameter range) nearly collisionless; $\mathbf{j}$ can then be written simply as

$$\mathbf{j}=eN_e(\mathbf{U}-\mathbf{u}_e), \tag{26}$$

the current being carried predominantly by the unimpeded electron flow velocity $\mathbf{u}_e$. Combining equation (24) with either (25) or (26) gives a relation between the disturbance magnetic field and the plasma and electron flow velocities, a relation independent of mode in the collisionless limit (the mode parameter $\sigma$ on both sides canceling out) but one that does depend on mode when collisions are important. It is this difference that accounts for the mode-dependent effect of collisions at low wave frequencies.

### 5.2. Resistivity Versus Neutral Drag

[28] In the conventional magnetosphere-ionosphere coupling theories, ideal MHD is used throughout the magnetosphere and Ohm's law is used in the height-integrated ionosphere. In contrast, our new results are obtained by adding dissipative effects throughout the whole system. There are several dissipative mechanisms, and here we look further into which one controls the coupling processes.

[29] We first examine Ohmic dissipation, which conventionally is viewed as the dominant mechanism. Ohmic dissipation can be easily studied from the conventional (resistive) magnetic induction equation, which can also be derived from equation (7) combined with some terms in equations (4) and (8),

$$\frac{\partial\mathbf{B}}{\partial t}=\nabla\times(\mathbf{U}\times\mathbf{B})+\frac{\zeta}{\mu_0}\nabla^2\mathbf{B}, \tag{27}$$

where $\zeta$ is the resistivity used in the conventional Ohm's law. Taking a time derivative and noticing that the first term on the right gives the Alfvén wave in the low-frequency limit, equation (27) is equivalent to

$$-\omega^2+k^2V_A^2-i\frac{\zeta}{\mu_0}k^2\omega=0 \tag{28}$$

or

$$\frac{\omega^2}{k^2}=V_A^2\left(1-i\frac{\omega\nu}{\Omega_i^2}\right), \tag{29}$$

where $\nu$ is the total collision frequency. It is clear that the resistivity effects on wave propagation are important only at high frequencies and become negligible at very low frequencies.

[30] We examine next the effect of neutral drag. As noted earlier, the plasma and neutral momentum equations can be simplified to the forms (16) and (17). The first term on the right of the plasma equation (16) gives the Alfvén wave. Eliminating the neutral velocity, the combination of the two equations is equivalent to

$$\left(-\omega^2+k^2V_A^2-i\nu_{in}\omega-\frac{\alpha\nu_{in}^2}{1+i\dfrac{\alpha\nu_{in}}{\omega}}\right)\mathbf{U}=0 \tag{30}$$

At low frequencies, the dispersion relation is

$$\frac{\omega^2}{k_R^2}=V_A^2\frac{\alpha\nu_{in}}{(1+\alpha)\nu_{in}} \tag{31}$$

and

$$\frac{k_I}{k_R}=\frac{\omega}{2\alpha\nu_{in}(1+\alpha)}. \tag{32}$$

Equation (31) gives the low-frequency limit of the phase velocity as shown in section 4. The numerator on the right is the neutral-ion collision frequency, $\nu_{ni}$, and the denominator is the ion-neutral collision frequency when $\alpha$ is much smaller than 1. The decrease in the phase velocity is due to the neutral-inertia loading process as discussed before. The mass ratio translates into the ratio of the neutral collision frequency to the ion collision frequency. Equation (32) is the attenuation rate at the low-frequency limit as discussed in section 4. Therefore the physical insight we learn from this analysis is that the controlling mechanism in the magnetosphere-ionosphere coupling at the lowest frequencies is properly described as neutral drag rather than as resistivity.

[31] The above statement brings to light a distinction that has not been made in most previous studies. Inputs of different types of energy into the ionosphere have been studied observationally [e.g., *Lu et al.*, 1995; *Fujii et al.*, 1998; *Thayer*, 2000] and questions have been raised, not about the inferred energy input rates but about the description of the physical mechanism of dissipation. A detailed discussion of energy transfer and dissipation in the ionosphere has been given by *Vasyliūnas and Song* [2005], who found, in a self-consistent three-fluid treatment, that distinguishing among kinetic energies of bulk flow, kinetic energies of relative flow, and thermal energies, as well as separating Ohmic or Joule heating from other types of energy input, turns out to be considerably more complicated than generally assumed. From a rigorous analysis both of the generalized Ohm's law and of the energy equations, *Vasyliūnas and Song* [2005] showed that Joule heating in the true sense is negligibly small and that the input magnetospheric energy is nearly equally distributed between the plasma and the neutrals by a collisional process. This process, although mathematically representable as Joule heating in some formulations, physically is

heating by friction between plasma and neutrals as a result of their relative bulk flow. Our results show that the general conclusion of Vasyliūnas and Song also applies to of wave propagation at very low frequencies and helps to understand some of its specific properties.

### 5.3. Nonuniformity

[32] The local uniformity approximation is one of the most restrictive assumptions in our analysis. There are two primary effects that violate it: vertical changes of ionospheric quantities and horizontal variations due to other forces. The latter may be accommodated to some extent by assuming that a steady state equation, involving the balance among the pressure gradient, Coriolis, and centrifugal forces, has been subtracted from each of (1), (2), and (3); then only the perturbed and not the initial plasma and neutral velocities must be assumed relatively uniform in the directions perpendicular to the propagation. As far as variations in the vertical direction are concerned, the local uniformity approximation holds if the wavelength is much shorter than the vertical scale of the gradients of the ionosphere, about $10^2$ km. As can be seen from Figure 3, this condition holds (and hence our model is quantitatively reliable) for the following frequency ranges: for the right-hand mode, from $\Omega_e$ down to 0.01 $\Omega_i$ at all heights and down to $10^{-4}$ $\Omega_i$ at 100 km; and for the left-hand mode, from $\Omega_i$ down to 0.01 $\Omega_i$ (but not at 100 km). Outside these ranges, our results are only qualitative at best. (Note: for the left-hand mode, the uniformity condition does not hold at all at 100 km except for frequencies above $\Omega_i$, which simply confirms that the left-hand mode does not occur at these frequencies: it does not propagate in the absence of collisions, and our conclusion that it is heavily damped in the presence of collisions is quantitatively valid at 100 km in any case.)

[33] Although the local uniformity approximation is not quantitatively satisfied in magnetosphere-ionosphere coupling, it is still widely used in analytical studies and data interpretations. Its applicability is in fact significantly improved by the neutral inertia loading and the consequent slowdown of the wave speed. We recall that the wavelength of the ULF waves can be comparable to the size of the magnetosphere if they propagate at the Alfvén speed. *Samson et al.* [1991, 1992] identified the magnetospheric fundamental modes to be 1.3 and 1.9 mHz. Using our parameters at 100 km in Table 2, the wave at 1.3 mHz corresponds to $\omega = 4.6 \times 10^{-5}\ \Omega_i$, the phase velocity for right-hand wave is 2.3 km/s and the wavelength is 1750 km, about 2 orders of magnitude smaller than that propagating at the Alfvén speed.

[34] For the right-hand mode at frequencies above the ion gyrofrequency, the damping is weak and the wavelength is short. The wave can penetrate through the ionosphere, which is consistent with the fact that whistlers are observed on the ground. However, as pointed out by *Kimura* [1966, 1985], the whistler waves may be reflected at the local lower-hybrid frequency when a nonzero propagation angle with respect to $\pm\mathbf{b}$ is allowed. Therefore interhemispheric traveling whistlers can also be explained.

[35] In addition to reflecting incident waves, vertical gradients also refract waves when the field line is not parallel to the gradients. In this case, a horizontal component of the wave will be generated, as pointed out by *Dungey* [1963] and treated by *Hughes and Southwood* [1973, 1976] and *Hughes* [1974] for the case without neutrals.

## 6. Conclusions

[36] We have developed a three-fluid wave description of the coupling from the solar wind to the magnetosphere and to the ionosphere and thermosphere, using a single set of equations with which the electric current, plasma velocity, neutral velocity, and electromagnetic field can be calculated as functions of space and time. As a first step, we have solved this equation set for an incompressible, locally uniform system and derived the dispersion relation for parallel propagation.

[37] Two important effects due to the presence of neutrals and their collisions with plasma have been identified. First, collisions with neutrals are equivalent to a neutral inertia loading process that makes the field line heavier and leads to a slowdown of the propagation, with the propagation speed at the lowest frequencies becoming the Alfvén speed based on the total mass density including the neutral mass. Second, there is damping of the perturbation due to the neutral collisions, at a rate that has been derived quantitatively as a function of frequency and collision frequencies as well as other plasma parameters. The damping is most pronounced for the left-hand mode and for higher frequencies.

[38] With this analysis of magnetosphere-ionosphere/thermosphere coupling we have shown that the coupling process is better described as a neutral drag process rather than Ohmic dissipation, contrary to widespread usage but in agreement with the recent independent and more detailed analysis of ionospheric energy equations by *Vasyliūnas and Song* [2005]. The coupling occurs only when there is relative motion between the neutral atmosphere and the plasma. There are two effects of this relative motion, as shown by Vasyliūnas and Song: energy dissipation occurs as frictional heating, which to first approximation is distributed equally between the plasma and the neutrals, and the entire magnetic stress is transferred to and must ultimately be balanced by the neutral atmosphere, most simply through accelerating the neutral flow (in the direction of plasma flow). In the coupled magnetosphere-ionosphere-thermosphere system, the neutral wind driven by the magnetospheric stress tends to reduce the ionospheric current and hence to reduce the total magnetospheric input power. The coupling process is thus time-dependent even when the plasma flow and associated enhanced electric field at the magnetopause or magnetotail (produced by reconnection) is constant for relatively long times.

[39] The present analysis is only the first step toward understanding time-dependent processes contained in this set of equations. Among the most urgent remaining tasks is relaxing some of the simplifying assumptions, particularly about the geometry.

## Appendix A: Derivation of Dispersion Relation

[40] Assume all the background parameters, such as densities and collision frequencies, are time-independent,

set $\mathbf{B}(t) = \mathbf{B}_0 + \delta\mathbf{B}(t)$, where $\delta B(t) \ll B_0$, and (in anticipation of the local uniformity approximation) neglect the curvature of the magnetic field. From Maxwell equations (7) and (8), eliminating $\mathbf{B}$, we relate $\mathbf{j}$ to $\mathbf{E}$,

$$\partial_t \mathbf{j} = -\frac{1}{\mu_0}\left(\nabla\times\nabla\times\mathbf{E} + \frac{1}{c^2}\partial_t^2\mathbf{E}\right). \tag{A1}$$

From (6), we have $\mathbf{u}_n$ in terms of $\mathbf{U}$,

$$\partial_t \mathbf{u}_n = \frac{B}{N_n m_n}\mathbf{j}\times\mathbf{b} - \frac{N_i m_i}{N_n m_n}\partial_t\mathbf{U} = \alpha\left(\frac{\Omega_i}{N_i e}\mathbf{j}\times\mathbf{b} - \partial_t\mathbf{U}\right), \tag{A2}$$

where $\mathbf{b}$ is the unit vector along the magnetic field. Substituting (A2) into (5) and eliminating $\mathbf{u}_n$, we obtain $\mathbf{U}$ in terms of $\mathbf{j}$,

$$\widehat{O}\,\partial_t\mathbf{U} = \frac{\Omega_i}{N_e e}\left[\partial_t\mathbf{j}\times\mathbf{b} + \alpha\nu_{in}\mathbf{j}\times\mathbf{b} + \frac{\nu_{en}-\nu_{in}}{\Omega_e}\partial_t\mathbf{j}\right], \tag{A3}$$

where for convenience we have defined

$$\widehat{O} \equiv \partial_t + (1+\alpha)\nu_{in}. \tag{A4}$$

Take the time derivative of (4) twice:

$$\begin{aligned}
\partial_t(4) \rightarrow \partial_t^2\mathbf{j} &= -\Omega_e\partial_t\mathbf{j}\times\mathbf{b} + N_e e\Omega_e\partial_t\mathbf{U}\times\mathbf{b} \\
&+ N_e e(\nu_{en}-\nu_{in})(\partial_t\mathbf{U} - \partial_t\mathbf{u}_n) - \nu_e\partial_t\mathbf{j} + \frac{N_e e^2}{m_e}\partial_t\mathbf{E} \\
&= -\Omega_e\partial_t\mathbf{j}\times\mathbf{b} + N_e e\Omega_e\partial_t\mathbf{U}\times\mathbf{b} + N_e e(\nu_{en}-\nu_{in})(1+\alpha)\partial_t\mathbf{U} \\
&- \alpha\Omega_i(\nu_{en}-\nu_{in})\mathbf{j}\times\mathbf{b} - \nu_e\partial_t\mathbf{j} + \frac{N_e e^2}{m_e}\partial_t\mathbf{E} \\
\partial_t^3\mathbf{j} &= -\Omega_e\partial_t^2\mathbf{j}\times\mathbf{b} + N_e e\Omega_e\partial_t^2\mathbf{U}\times\mathbf{b} + N_e e(\nu_{en}-\nu_{in})(1+\alpha)\partial_t^2\mathbf{U} \\
&- \alpha\Omega_i(\nu_{en}-\nu_{in})\partial_t\mathbf{j}\times\mathbf{b} - \nu_e\partial_t^2\mathbf{j} + \frac{N_e e^2}{m_e}\partial_t^2\mathbf{E}
\end{aligned}$$

Substitute (A2) and (A3) into the above equation and eliminate $\mathbf{U}$ and $\mathbf{u}_n$ to obtain an equation for $\mathbf{j}$ and $\mathbf{E}$,

$$\begin{aligned}
\widehat{O}\,\partial_t^3\mathbf{j} &= -\Omega_e\,\widehat{O}\,\partial_t^2\mathbf{j}\times\mathbf{b} - \alpha\Omega_i(\nu_{en}-\nu_{in})\,\widehat{O}\,\partial_t\mathbf{j}\times\mathbf{b} - \nu_e\,\widehat{O}\,\partial_t^2\mathbf{j} \\
&+ \frac{N_e e^2}{m_e}\,\widehat{O}\,\partial_t^2\mathbf{E} + \Omega_i\Omega_e\left[\partial_t^2\mathbf{j}\times\mathbf{b} + \alpha\nu_{in}\partial_t\mathbf{j}\times\mathbf{b}.\right. \\
&\left. + \frac{(\nu_{en}-\nu_{in})}{\Omega_e}\partial_t^2\mathbf{j}\right]\times\mathbf{b} + (1+\alpha)\Omega_i(\nu_{en}-\nu_{in}) \\
&\cdot\left[\partial_t^2\mathbf{j}\times\mathbf{b} + \alpha\nu_{in}\partial_t\mathbf{j}\times\mathbf{b} + \frac{(\nu_{en}-\nu_{in})}{\Omega_e}\partial_t^2\mathbf{j}\right]
\end{aligned} \tag{A5}$$

Express (A5) in terms of $\partial_t\mathbf{j}$, $\partial_t\mathbf{j}\times\mathbf{b}$,

$$\begin{aligned}
&\left[\widehat{O}\,\partial_t^2 + \nu_e\,\widehat{O}\,\partial_t - (1+\alpha)\frac{\Omega_i(\nu_{en}-\nu_{in})^2}{\Omega_e}\partial_t\right]\partial_t\mathbf{j} \\
&+ \left[\Omega_e\,\widehat{O}\,\partial_t + \alpha\Omega_i(\nu_{en}-\nu_{in})\,\widehat{O} - (2+\alpha)\Omega_i(\nu_{en}-\nu_{in})\partial_t\right. \\
&\left. - (1+\alpha)\alpha\Omega_i\nu_{in}(\nu_{en}-\nu_{in})\right]\partial_t\mathbf{j}\times\mathbf{b} \\
&- \Omega_i\Omega_e[\partial_t + \alpha\nu_{in}](\partial_t\mathbf{j}\times\mathbf{b})\times\mathbf{b} = \frac{N_e e^2}{m_e}\,\widehat{O}\,\partial_t^2\mathbf{E}
\end{aligned} \tag{A6}$$

Now substitute (A2) into (A6) to obtain an equation for $\mathbf{E}$:

$$\begin{aligned}
&\left[\widehat{O}\,\partial_t^2 + \nu_e\,\widehat{O}\,\partial_t - (1+\alpha)\frac{\Omega_i(\nu_{en}-\nu_{in})^2}{\Omega_e}\partial_t\right] \\
&\cdot\left(\nabla\times\nabla\times\mathbf{E} + \frac{1}{c^2}\partial_t^2\mathbf{E}\right) + \left[\Omega_e\,\widehat{O}\,\partial_t + \alpha\Omega_i(\nu_{en}-\nu_{in})\,\widehat{O}\right. \\
&\left. - (2+\alpha)\Omega_i(\nu_{en}-\nu_{in})\partial_t - (1+\alpha)\alpha\Omega_i\nu_{in}(\nu_{en}-\nu_{in})\right] \\
&\cdot\left(\nabla\times\nabla\times\mathbf{E} + \frac{1}{c^2}\partial_t^2\mathbf{E}\right)\times\mathbf{b} - \Omega_i\Omega_e(\partial_t + \alpha\nu_{in}) \\
&\cdot\left[\left(\nabla\times\nabla\times\mathbf{E} + \frac{1}{c^2}\partial_t^2\mathbf{E}\right)\times\mathbf{b}\right]\times\mathbf{b} = -\frac{\mu_0 N_e e^2}{m_e}\,\widehat{O}\,\partial_t^2\mathbf{E}
\end{aligned} \tag{A7}$$

Under our assumption of parallel propagation, the parallel component of (A7) gives an equation for $E_\parallel$ that describes pure oscillations at the electron plasma frequency, decoupled from propagating modes. Leaving them aside, the conditions of $\nabla\bullet\mathbf{E} = 0$ and $\mathbf{E}\bullet\mathbf{b} = 0$ hold for the remaining transverse waves, and (noting that $\mu_0 N_e e^2/m_e = \omega_{pe}^2/c^2$) (A7) becomes

$$\begin{aligned}
&\left[\widehat{O}\,\partial_t^2 + \nu_e\,\widehat{O}\,\partial_t - (1+\alpha)\frac{\Omega_i(\nu_{en}-\nu_{in})^2}{\Omega_e}\partial_t + \Omega_i\Omega_e(\partial_t + \alpha\nu_{in})\right] \\
&\cdot\left(\nabla^2\mathbf{E} - \frac{1}{c^2}\partial_t^2\mathbf{E}\right) - \frac{\omega_{pe}^2}{c^2}\,\widehat{O}\,\partial_t^2\mathbf{E} \\
&+ \left[\Omega_e\,\widehat{O}\,\partial_t + \alpha\Omega_i(\nu_{en}-\nu_{in})\,\widehat{O} - (2+\alpha)\Omega_i(\nu_{en}-\nu_{in})\partial_t\right. \\
&\left. - (1+\alpha)\alpha\Omega_i\nu_{in}(\nu_{en}-\nu_{in})\right]\left(\nabla^2\mathbf{E} - \frac{1}{c^2}\partial_t^2\mathbf{E}\right)\times\mathbf{b} = 0
\end{aligned} \tag{A8}$$

or

$$\widehat{C}_1\,\mathbf{E} + \widehat{C}_2\,\mathbf{E}\times\mathbf{b} = 0 \tag{A9}$$

where

$$\begin{aligned}
\widehat{C}_1(\mathbf{r},\partial_t,\nabla) &= \left[\widehat{O}\,\partial_t^2 + \nu_e\,\widehat{O}\,\partial_t - (1+\alpha)\frac{\Omega_i(\nu_{en}-\nu_{in})^2}{\Omega_e}\partial_t\right. \\
&\left. + \Omega_i\Omega_e(\partial_t + \alpha\nu_{in})\right]\left(\nabla^2 - \frac{1}{c^2}\partial_t^2\right) - \frac{\omega_{pe}^2}{c^2}\,\widehat{O}\,\partial_t^2 \\
\widehat{C}_2(\mathbf{r},\partial_t,\nabla) &= \left[\Omega_e\,\widehat{O}\,\partial_t + \alpha\Omega_i(\nu_{en}-\nu_{in})\,\widehat{O}\right. \\
&- (2+\alpha)\Omega_i(\nu_{en}-\nu_{in})\partial_t \\
&\left. -(1+\alpha)\alpha\Omega_i\nu_{in}(\nu_{en}-\nu_{in})\right]\left(\nabla^2 - \frac{1}{c^2}\partial_t^2\right)
\end{aligned} \tag{A10}$$

In Cartesian coordinates with the z-axis along the magnetic field, the component form of (A9) is

$$\begin{cases}
\widehat{C}_1\,E_x + \widehat{C}_2\,E_y = 0 \\
\widehat{C}_1\,E_y - \widehat{C}_2\,E_x = 0
\end{cases} \tag{A11}$$

Defining, for convenience, the left/right polarization fields,

$$\mathbf{E}_\pm = \mathbf{E}_x \pm i\mathbf{E}_y, \quad \widehat{C}_\pm = \widehat{C}_1 \pm i\,\widehat{C}_2 \tag{A12}$$

(A11) becomes

$$\widehat{C}_{\mp}\,\mathbf{E}_{\pm} = 0 \tag{A13}$$

and

$$\begin{aligned}\widehat{C}_{\pm}(\mathbf{r},\partial_t,\nabla) = &\left[\widehat{O}\,\partial_t^2 + \nu_e\,\widehat{O}\,\partial_t - (1+\alpha)\frac{\Omega_i(\nu_{en}-\nu_{in})^2}{\Omega_e}\partial_t\right.\\ &\left.+\,\Omega_i\Omega_e(\partial_t+\alpha\nu_{in})\right]\left(\nabla^2-\frac{1}{c^2}\partial_t^2\right) - \frac{\omega_{pe}^2}{c^2}\widehat{O}\,\partial_t^2\\ &\pm i\Big[\Omega_e\,\widehat{O}\,\partial_t + \alpha\Omega_i(\nu_{en}-\nu_{in})\,\widehat{O} - (2+\alpha)\Omega_i(\nu_{en}-\nu_{in})\partial_t\\ &-(1+\alpha)\alpha\Omega_i\nu_{in}(\nu_{en}-\nu_{in})\Big]\left(\nabla^2-\frac{1}{c^2}\partial_t^2\right)\end{aligned} \tag{A14}$$

Since there is no explicit time dependence, we Fourier-decompose (A14) in time, using

$$\mathbf{E}_{\pm}(\mathbf{r},t) = \mathbf{E}_{\pm 0}(\mathbf{r},\omega)e^{i\omega t} \tag{A15}$$

whence $\widehat{O}\,(\mathbf{r},\,i\omega) \equiv i\omega + \nu_{in}(1+\alpha)$,

$$\begin{aligned}\widehat{C}_{\pm}(\mathbf{r},i\omega,\nabla) = &\,\Omega_e\Omega_i[i\omega+\nu_{in}(1+\alpha)]\\ &\cdot\left\{\left[-\frac{\omega^2}{\Omega_e\Omega_i}\mp\frac{\omega}{\Omega_i}+1+i\frac{\omega\nu_e}{\Omega_e\Omega_i}\pm i\alpha\frac{(\nu_{en}-\nu_{in})}{\Omega_e}\right.\right.\\ &\left.\left.-\frac{(1+\alpha)\frac{(\nu_{en}-\nu_{in})^2}{\Omega_e^2}\pm\alpha(1+\alpha)\frac{(\nu_{en}-\nu_{in})\nu_{in}}{\omega\Omega_e}-i\frac{\nu_{in}}{\omega}\pm i(2+\alpha)\frac{(\nu_{en}-\nu_{in})}{\Omega_e}}{1-i(1+\alpha)\frac{\nu_{in}}{\omega}}\right]\right.\\ &\left.\cdot\left(\nabla^2+\frac{\omega^2}{c^2}\right)+n_A^2\frac{\omega^2}{c^2}\right\}\end{aligned} \tag{A16}$$

where $n_A = c/V_A$.

Divided by the nonzero quantity $\Omega_e\Omega_i\hat{O}(\mathbf{r},\,i\omega)$, the operator (A16) turns (A13) into the simple differential equation

$$\left[f_{\mp}(\mathbf{r},\omega)\left(\nabla^2+\frac{\omega^2}{c^2}\right)-n_A^2\frac{\omega^2}{c^2}\right]\mathbf{E}_{\pm}(\mathbf{r},\omega) = 0 \tag{A17}$$

or

$$\left[\nabla^2+\frac{\omega^2}{c^2}\left(1-\frac{n_A^2}{f_{\mp}(\mathbf{r},\omega)}\right)\right]\mathbf{E}_{\pm}(\mathbf{r},\omega) = 0 \tag{A18}$$

where

$$\begin{aligned}f_{\pm}(\mathbf{r},\omega) = &\frac{\omega^2}{\Omega_e\Omega_i}\pm\frac{\omega}{\Omega_i}-1-i\frac{\omega\nu_e}{\Omega_e\Omega_i}\mp i\alpha\frac{\nu_{en}-\nu_{in}}{\Omega_e}\\ &+\frac{(1+\alpha)\frac{(\nu_{en}-\nu_{in})^2}{\Omega_e^2}\pm\alpha(1+\alpha)\frac{(\nu_{en}-\nu_{in})\nu_{in}}{\omega\Omega_e}-i\frac{\nu_{in}}{\omega}\pm i(2+\alpha)\frac{\nu_{en}-\nu_{in}}{\Omega_e}}{1-i(1+\alpha)\frac{\nu_{in}}{\omega}}\end{aligned} \tag{A19}$$

Under our approximation of a locally homogeneous medium, the spatial gradients of all the background parameters can be neglected:

$$\begin{aligned}\nabla\nu_{en} = \nabla\nu_{ei} = \nabla\nu_{in} = \nabla N_e = \nabla m_i = \nabla N_n\\ = \nabla m_n = \nabla\Omega_e = \nabla\Omega_i = 0\end{aligned} \tag{A20}$$

We then Fourier-decompose (18) in space, using

$$\mathbf{E}_{\pm}(\mathbf{r}) = \mathbf{E}_{\pm 0}(k)e^{-i\mathbf{k}_{\pm}\mathbf{r}} \tag{A21}$$

$$-k_{\pm}^2+\frac{\omega^2}{c^2}\left(1-\frac{n_A^2}{f_{\mp}(\omega)}\right) = 0, \qquad f_{\mp}(\omega) = \frac{n_A^2}{1-\frac{c^2k_{\pm}^2}{\omega^2}} = \frac{n_A^2}{1-n_{\pm}^2}$$

Combining this with (A19), we finally obtain the dispersion relation

$$\begin{aligned}&\left[\frac{\omega^2}{\Omega_e\Omega_i}\pm\frac{\omega}{\Omega_i}-1+(1+\alpha)\frac{(\nu_{en}-\nu_{in})^2}{\Omega_e^2}-(1+\alpha)\frac{\nu_{in}\nu_e}{\Omega_e\Omega_i}\right]\\ &\quad-i\left[\frac{\omega\nu_e}{\Omega_e\Omega_i}+(1+\alpha)\frac{\omega\nu_{in}}{\Omega_e\Omega_i}\pm(1+\alpha)\frac{\nu_{in}}{\Omega_i}\mp2\frac{\nu_{en}-\nu_{in}}{\Omega_e}-\alpha\frac{\nu_{in}}{\omega}\right]\\ &\quad=\frac{n_A^2}{1-n_{\mp}^2}\left[1-i(1+\alpha)\frac{\nu_{in}}{\omega}\right]\end{aligned} \tag{A22}$$

where $n = ck/\omega$.

[41] **Acknowledgments.** We thank R. Boström, M. G. Kivelson, A. Richmond, and D. Shklyar for their valuable comments and physical insights. The work was supported by NSF under Award NSF-ATM0318643.

[42] Arthur Richmond thanks Anatoly V. Streltsov and another reviewer for their assistance in evaluating this paper.

## References

Akasofu, S.-I., and R. N. Dewitt (1965), Dynamo action in the ionosphere and motions of the magnetospheric plasma III. The Pedersen conductivity, generalized to take account of acceleration of the neutral gas, *Planet. Space Sci.*, *13*, 737.

Booker, H. G. (1984), *Cold Plasma Waves*, Springer, New York.

Boström, R. (1974), Ionosphere-magnetosphere coupling, in *Magnetospheric Physics*, edited by B. M. McCormac, pp. 45, Springer, New York.

Brillouin, L. (1960), *Wave Propagation and Group Velocity*, Elsevier, New York.

Dungey, J. W. (1963), Hydromagnetic waves and the ionosphere, in *Proceedings of International Conference on the Ionosphere*, *Rep. 230*, Inst. of Phys., London.

Fujii, R., S. Nozawa, S. C. Buchert, and A. Brekke (1998), Statistical characteristics of electromagnetic energy transfer between the magnetosphere, the ionosphere and the thermosphere, *J. Geophys. Res.*, *104*, 2357.

Gombosi, T. I. (1994), *Gaskinetic Theory*, Cambridge Univ. Press, New York.

Hughes, W. J. (1974), The effect of the atmosphere and ionosphere on long period magnetospheric micropulsations, *Planet. Space Sci.*, *22*, 1157.

Hughes, W. J., and D. J. Southwood (1973), Effect of atmosphere and ionosphere on magnetospheric micropulsation signals, *Nature*, *248*, 493.

Hughes, W. J., and D. J. Southwood (1976), The screening of micropulsation signals by the atmosphere and ionosphere, *J. Geophys. Res.*, *81*, 3234.

Kelley, M. C. (1989), *The Earth's Ionosphere: Plasma Physics and Electrodynamics*, Elsevier, New York.

Kimura, I. (1966), Effects of ions on whistler-mode ray tracing, *Radio Sci.*, *1*(3), 269.

Kimura, I. (1985), Whistler mode propagation in the Earth and planetary magnetospheres and ray tracing techniques, *Space Sci. Rev.*, *42*(3/4), 449.

Lu, G., A. D. Richmond, B. A. Emery, and R. G. Roble (1995), Magnetosphere-ionosphere-thermosphere coupling: Effect of neutral winds on the energy transfer and field aligned current, *J. Geophys. Res.*, *100*, 19,643.

Lysak, R. L. (1990), Electrodynamic coupling of the magnetosphere and ionosphere, *Space Sci. Rev.*, *52*, 33.

Lysak, R. L. (1999), Propagation of Alfvén waves through the ionosphere: Dependence on ionospheric parameters, *J. Geophys. Res.*, *104*, 10,017.

Peymirat, C., A. D. Richmond, B. A. Emery, and R. G. Roble (1998), A magnetosphere-thermosphere-ionosphere electrodynamics general circulation model, *J. Geophys. Res.*, *103*, 17,467.

Richmond, A. D., E. C. Ridley, and R. G. Roble (1992), A thermosphere/ionosphere general circulation model with coupled electrodynamics, *Geophys. Res. Lett.*, *19*, 601.

Roble, R. G., E. C. Ridley, A. D. Richmond, and R. E. Dickinson (1998), A coupled thermosphere/ionosphere general circulation model, *Geophys. Res. Lett.*, *15*, 1325.

Samson, J. C., T. J. Hughes, F. Creutzberg, D. D. Wallis, R. A. Greenwald, and J. M. Ruohoniemi (1991), Observations of a detached, discrete arc in association with field line resonances, *J. Geophys. Res.*, *96*, 15,683.

Samson, J. C., D. D. Wallis, T. J. Hughes, F. Creutzberg, J. M. Ruohoniemi, and R. A. Greenwald (1992), Substorm intensification and field line resonances in the nightside magnetosphere, *J. Geophys. Res.*, *97*, 8495.

Schunk, R. W., and A. F. Nagy (2000), *Ionospheres*, Cambridge Univ. Press, New York.

Sen, H. K., and A. A. Wyller (1960), On the generalization of the Appleton-Hartree magnetoionic formulas, *J. Geophys. Res.*, *65*, 3931.

Song, P., and V. M. Vasyliūnas (2002), Solar wind-magnetosphere-ionosphere coupling: Signal arrival time and perturbation relations, *J. Geophys. Res.*, *107*(A11), 1358, doi:10.1029/2002JA009364.

Song, P., T. I. Gombosi, and A. D. Ridley (2001), Three-fluid Ohm's law, *J. Geophys. Res.*, *106*, 8149.

Song, P., V. M. Vasyliūnas, and L. Ma (2005), A three-fluid model of solar wind- magnetosphere-ionosphere-thermosphere coupling, in *Multiscale Coupling of Sun-Earth Processes*, edited by A. T. Y. Lui, Y. Kamide, and G. Consolini, pp. 447–456, Elsevier, New York.

Strangeway, R. J. (2002), Energy transmission through the ionosphere, *Eos. Trans. AGU*, *83*(19), Spring Meet. Suppl., Abstract SM 41C-07.

Thayer, J. P. (2000), High-latitude currents and their energy exchanges with the ionosphere-thermosphere system, *J. Geophys. Res.*, *105*, 23,015.

Vasyliūnas, V. M., and P. Song (2005), Meaning of ionospheric Joule heating, *J. Geophys. Res.*, *110*, A02301, doi:10.1029/2004JA010615.

L. Ma and P. Song, Center for Atmospheric Research and Department of Environmental, Earth, and Atmospheric Sciences, University of Massachusetts-Lowell, 600 Suffolk Street, Lowell, MA 01854, USA. (paul_song@uml.edu)

V. M. Vasyliūnas, Max-Planck-Institut für Sonnensystemforschung, D-37191 Katlenburg-Lindau, Germany.